PAPER Nr. : 63

DESIGN AND DEVELOPMENT OF A DYNAMICALLY SCALED MODEL AH-64 MAIN ROTOR

F.K. STRAUB, R.A. JOHNSTON, R.E. HEAD
HUGHES HELICOPTERS, INC.
CULVER CITY, CALIFORNIA

H.L. KELLEY
U.S. ARMY RESEARCH AND TECHNOLOGY LABORATORIES (AVSCOM)
HAMPTON, VIRGINIA

TENTH EUROPEAN ROTORCRAFT FORUM

AUGUST 28 – 31, 1984 – THE HAGUE, THE NETHERLANDS

DESIGN AND DEVELOPMENT OF A DYNAMICALLY SCALED MODEL AH-64 MAIN ROTOR

F.K. Straub, R.A. Johnston, R.E. Head
Hughes Helicopters, Inc.
Culver City, California

H.L. Kelley
U.S. Army Research and Technology Laboratories (AVSCOM)
Hampton, Virginia

ABSTRACT

A 27% dynamically scaled model of the AH-64 Apache Advanced Attack Helicopter has been designed and developed by Hughes Helicopters, Inc. This work was performed under contract to the Structures Laboratory, U.S. Army Research and Technology Laboratories (AVSCOM). Hughes Helicopters, Inc. (HHI) designed the model rotor and fabricated the rotor hub. The model rotor blades were fabricated by TM Development, Inc. All the dynamic and aeroelastic analyses were conducted at HHI. The 13-foot-diameter model has undergone a series of performance tests in the NASA Langley Research Center 4x7 meter V/STOL wind tunnel where full-scale flight conditions were simulated. The rotor was mounted on the General Rotor Model System (GRMS), with a scaled AH-64 fuselage shell around the GRMS for complete helicopter simulation. These tests will provide a better understanding of the current Apache rotor and, together with testing of advanced rotor blade designs, will suggest potential improvements in the blade design for the AH-64 Apache. This paper describes the design of the model rotor, its dynamic and aeroelastic properties as compared to the full scale rotor, and the model rotor integration with the GRMS. In particular, the coupled rotor/GRMS aeromechanical behavior is addressed, and steps to eliminate a potential instability are discussed.

1. INTRODUCTION

Wind tunnel testing of model rotors is an extremely useful tool for the development of new and improved helicopter rotor systems. It also provides valuable data for validation of analysis codes. As compared to full scale flight testing, model rotors offer cost and time savings in the development, as well as

during testing. Futhermore, wind tunnel testing is relatively safe. Because of the lower risk, exploration of flight conditions well beyond full scale operating limits is feasible. The wind tunnel environment also permits testing under closely controlled conditions, and thereby insures repeatability of any particular test point.

The primary thrust of model rotor testing in the past has been directed towards improving rotor performance. There are numerous studies that have investigated performance gains due to use of advanced airfoils and changes in blade geometry such as twist, planform, and tip shape. Recent advances in composite material technology now permit construction of model rotor blades with scaled dynamic properties. As a result, rotor loads, vibration, and stability can now be predicted from scale model tests.

The NASA Langley V/STOL tunnel and the General Rotor Model System (GRMS) are particularly suited for investigating the characteristics of lifting rotor systems[1]. The closed-return atmospheric tunnel is capable of producing forward speeds up to 200 knots. The test section is 14.5 ft. (4.42 m) high by 21.75 ft. (6.63 m) wide. Hover testing is usually performed by raising the ceiling and both side walls. To simulate hover out of ground effect conditions the floor can be lowered. The GRMS is supported on a unique sting, the high alpha-beta sting. The sting, by movement of three joints simultaneously, keeps the model at a fixed point in the tunnel while sweeping angle of attack on sideslip through a range of $\pm$ 45°. In addition, the tunnel has relatively low background noise, and has been used for rotor acoustic testing.

Rotor models are tested on the General Rotor Model System. The GRMS is a complex arrangement of internal balances, rotor drive and control systems. The rotor is directly attached to the drive shaft. The rotor, swashplate control, two electric drive motors, and transmission are supported on a six component strain-gage balance. This provides accurate measurements of rotor forces and moments. The rotor balance itself is connected to the GRMS structure through a soft, damped, gimbaled frame which permits roll and pitch motions. Some variation of hub impedance is possible through changes in the gimbal spring and damping properties. This is particularly useful for dealing with potential ground resonance problems. For complete helicopter simulation a scaled fuselage is fitted around the GRMS structure with an additional balance measuring the total model loads.

The AH-64 Apache Advanced Attack Helicopter (AAH) has recently been put into production and will be entering the U.S.

Army inventory in the near future. Many technological advances were incorporated in the rotor system and dynamic components[2]. These include the advanced HH-02 airfoil and a swept tip on the main rotor blade, a fully articulated main rotor with tension-torsion strap blade retention, a static main rotor mast and a tuned airframe.

Under contract Hughes Helicopters developed a 27% dynamically Mach scaled model of the AH-64 main rotor. The model rotor hub is shown in Figure 1. This rotor has been tested in the Langley V/STOL tunnel using the GRMS. A 27% scale AH-64 fuselage shell was developed separately at Langley. The complete model, installed in the V/STOL tunnel, is shown in Figure 2. At the same time, NASA Langley procured a set of advanced AH-64 rotor blades to verify the aerodynamic design methods discussed in Reference 3. The objectives of the test were to provide a data base for the evaluation of the baseline and advanced AH-64 rotor systems. In order to permit investigation of performance, rotor dynamics and acoustic improvements, dynamic Mach scaling was required.

The model hub has all the features of the full-scale hub, including the laminated steel strap blade retention system and elastomeric damper restraint for the lead-lag motion. The blades are molded to shape from advanced composite materials. This paper describes the scaling requirements and the design of the model rotor hub and blades, as well as the instrumentation provided with them.

The main body of the paper deals with the dynamic analysis of the model rotor and its integration with the GRMS. The full scale AAH main rotor has been tested extensively, and has been demonstrated to have excellent dynamic characteristics. HHI has conducted a number of studies to guide the design of the model rotor. These studies have resulted in a model rotor with dynamic characteristics that closely match those of the full scale rotor. There are, nevertheless, a number of important issues that had to be addressed. No attempt has been made to scale the dynamic properties of the GRMS to those of the AAH airframe and control system. For this reason, scaled behavior of the coupled rotor/fuselage is essentially lost when the model rotor is mounted on the GRMS.

Integrating any rotor with any fixed structure always produces the possibility of adverse coupling among the two that can lead to aeromechanical or aeroelastic problems or excessive forced responses. This is particularly true for ground resonance since it is not possible to "fly out" of a problem as is generally the case with an actual rotorcraft. The steps taken to assure safe testing of the model AAH rotor without encountering aeromechanical instability are discussed in detail in the paper.

2. SCALING REQUIREMENTS

Scaling first of all requires that the model rotor have similar geometry as the full scale rotor. That is, the hub geometry, blade planform, built in twist, and airfoil contours must be exactly scaled. The length scale factor, S, is determined by the size of the tunnel test section which must accomodate the model rotor. For the AH-64 model S=0.27 was chosen. This results in a 13 foot diameter rotor (the test section is 21.75 ft. wide).

Aerodynamic similarity is governed by three nondimensional parameters, namely Mach, Froude and Reynolds numbers. In general, for the same fluid medium, only one of these parameters can be matched. The choice depends on the objectives of the test. For rotor performance testing Mach number similarity is necessary since it results in similar aerodynamic loading. For Mach similarity in air, the time scale is identical to the length scale. The AH-64 model rotor speed is thus 1070 rpm, resulting in full scale tip speed of 735 fps. Froude similarity is only important when the helicopter stability and response to control inputs is considered. Reynolds number similarity in contrast to fixed wing testing is of less importance for rotor testing. The effects of reduced Reynolds number for Mach scaled rotors is discussed in Reference 4.

Finally, the rotor lock number must be matched for the model. This requires scaling the blade flapping inertia. From this the scale factor for the rotor mass properties is found as S^3. Scaling of forces can then be derived; forces are scaled by S^2. A summary of the basic scale factors for the AH-64 model is shown in Table 1.

Table 1: Scale Factors for Mach Scaling in Air

Length	S=0.27	Time	S
Mach Number	1	Mass	S^3
Lock Number	1	Force	S^2

The above describes the basic scaling requirements for model rotor performance testing. In addition, a rotor is said to be dynamically or aeroelastically scaled if its stiffness and mass distributions as well as the blade cross-sectional offsets are correctly scaled. This will result in similar model blade elastic twist and thereby improve correlation with full-scale performance data. In addition, blade elastic loads, vibrations, and aeroelastic stability can then be directly scaled. In general advanced composite materials are required to tailor the

properties of the model blades and achieve dynamic similarity. Dynamic scaling was the approach chosen for the AH-64 model rotor.

3. DESIGN OF THE MODEL ROTOR

In this section the design features of the model AH-64 rotor are discussed. The rotor was required to have 5% overspeed capability at wind speeds of up to 160 Knots. Design of the hub was a particularly challenging task. As is apparent from Table 1, stresses remain constant with dynamic Mach scaling, whereas mass is scaled by the cube of the scale factor. Therefore, several iterations had to be made to arrive at a design that would satisfy the dynamic scaling requirements and yet provide the necessary static and fatigue strengths. Dynamic analysis was used extensively to guide the rotor design. It should also be noted here that no attempt was made to compensate in the rotor design for differences in the hub support of the AH-64 as compared to the GRMS. A summary of the AH-64 main rotor properties is given in Table 2.

Table 2: AH-64 Main Rotor Geometry

	Full Scale		27% Model	
Number of Blades	4		4	
Rotor Radius	288	in.	77.76	in.
Blade Flap Hinge Offset	11	in.	2.97	in.
Blade Lag Hinge Offset	34.5	in.	9.32	in.
Nominal Rotor Speed	289	rpm	1070	rpm
Blade Chord	21	in.	5.67	in.
Blade Tip Sweep (from 0.93R)	20°		20°	
Blade Twist	-9°		-9°	

3.1 MODEL ROTOR HUB

The model rotor hub has all the features of the full-scale rotor. The major hub components are shown in Figure 3. On the AH-64 helicopter, the hub is supported by a pair of tapered roller bearings running on a stationary mast. This mast carries all rotor loads, while a separate drive shaft transmits torque to the rotor. In contrast, the model rotor hub is directly attached to the GRMS drive shaft.

The center piece of the hub consists of an upper and lower hub shoe. The blade retention straps are clamped between the two hub shoes. The centrifugal loads are shared by the hub shoes; all

other loads are carried by the upper shoe. The upper hub shoe also provides guiding for the flap motion of the blade retention straps and contains the splined interface for mounting to the GRMS drive shaft. Both hub shoes were machined from 4030 steel. This resulted in a significantly heavier than ideally scaled hub, see Table 3. Other materials were considered. However, analysis showed that only minor improvements in dynamic scaling would have been achieved.

The stainless steel retention straps connect the blades to the hub. Their laminated construction and truss-like planform provide flexibility to accomodate the blade flap and feathering motion and inplane stiffness to transmit the drive torque. Since scaling of the laminate thickness was not practical, a reduction in the number of laminates by half was chosen. This permitted use of the same laminate sheets as on the Hughes Model 500 helicopter. This material also provided higher ultimate strength and fatigue allowables than the material used for the AH-64 straps. Furthermore, by eliminating the non-structural interlaminate material the strap pack structural area was increased, resulting in acceptable fatigue factors. As a result of this, however, the strap pack inplane stiffness is 19% higher than ideally scaled. The final strap pack consisted of 11 laminates, each 0.009 inch thick.

The pitch housing encloses the strap pack and transmits the feathering input to the blade. The inboard end of the pitch housing is centered by the pitch horn assembly which includes the flap/feather bearing and the droop stop. Both parts were machined from high grade aluminum alloy. Since the full-scale parts are aluminum castings, strength factors were sufficiently high. However, wall thickness became a limiting factor and resulted in a heavier than scaled pitch housing. The lead-lag fitting provides the blade attachment lugs and connects to the pitch housing through a teflon lined bearing which permits blade inplane motion. This link was also machined from aluminum alloy and treated by shot-peening. The model elastomeric blade lead-lag dampers, two per blade, were manufactured by Barry Controls, with the dynamic stiffness and damping properties within tolerance of the appropriately scaled full-scale values. All of the above components constitute the 'flapping hardware'. Considerable effort was spent to reduce the weight of this group from its initial value of 3.44 lbs. Dynamic analysis showed that the heavier than scaled flapping hardware resulted in a lowering of the flap bending mode frequencies. Practical size limitations prevented a weight reduction below the 2.68 lbs. shown in Table 3.

Significant differences exist between the AH-64 control system and that of the GRMS. The GRMS swashplate support and

screw-type mechanical actuators, which are driven by three small electric motors, result in a much higher control system stiffness than that of the AH-64. To compensate somewhat for this, modified S-shape pitch links were designed, resulting in a lower pitch link stiffness than would have been possible with a straight pitch link. The control system stiffness values shown in Table 3 are average values of the longitudinal and lateral cyclic stiffness values obtained from applying twisting moments at the blade root.

Table 3: Hub Data Comparison - 0.27 Scale Rotor

	Ideally Scaled	27% Model
Hub Weight - lb.	3.29	6.55
Flapping Hardware		
Wt. - lb.	2.06	2.68
C.G. - in. from Centerline	6.95	6.66
I_θ - lb.-in.^{2}	2.63	3.77
Strap Chordwise Stiffness - lb./in.	7695.	9157.
Control System Stiffness - $\frac{\text{lb.-in.}}{\text{rad.}}$	6950.	13,300.

The hub instrumentation consists of two displacement transducers. One is mounted on the upper hub shoe and provides flap angle measurements. The second transducer is mounted on one of the lead-lag dampers and provides lead-lag angle readouts.

3.2 MODEL BLADES

To meet the demanding requirements of dynamic Mach scaling the model AH-64 blades were fabricated from advanced composite materials. The cross-section of the blade is shown in Figure 4. The blades are formed to shape by use of an aluminum mold. The mold exactly represents the scaled planform, including the 20° tip sweep outboard of 0.93R, and the contour of the HH02 cambered airfoil with its trailing edge tab. Blade pretwist is generated by twisting the mold to -9° linear pretwist before lay-up of the blade.

The blade is built up from a graphite/epoxy prepreg torsion box ($\pm$ 45°) which is reinforced with unidirectional fore and aft graphite spars (0°). The spar tube is filled with foam (6 lb./ft.^{3}). The foam is machined in two halves so that a fiberglass conduit can be inserted. This conduit carries the

strain gage wiring. The trailing edge core consists of machined foam (2 lb./ft.^{3}), and balsa wood ribs with 90° graphite caps, spaced three inches apart radially. The outer blade skin consists of Kevlar-49/epoxy prepreg (0°/90°). The trailing edge tab is reinforced with graphite stiffener (90°). The proper chordwise C.G. balance is obtained by including brass wire packs in the leading edge. The tip weight of 0.059 lb. is similarly constructed from brass wire packs. The two blade attach bushings are made of titanium and are wrapped with graphite loops to carry the centrifugal loads.

A number of blade test articles were fabricated to arrive at the correctly scaled blade properties and to test for structural integrity and sufficient strength factors. The final blade properties are given in Table 4. The chordwise and flapwise stiffness distributions and the mass distributions are very well scaled. The torsional stiffness is high by 20%. This was expected to have only a small effect on the elastic twist and little effect on the lowest torsion mode dynamics (the GRMS control system stiffness is considerably higher than the scaled value). The blade cross-sectional offsets, namely elastic axis, chordwise C.G., and aerodynamic center location are also very well scaled. The feathering axis, by design, is located at 27% chord, identical to the full-scale value. Note that distributed parameter values in Table 4 are given for the uniform blade section.

Table 4: Blade Data Comparison - 27% Scale Rotor

	Ideally Scaled	27% Model
EI_c	4.55 x 10^6 lb.-in.^{2}	4.44 x 10^6
EI_f	109,500 "	106,950
GJ	101,000 "	124,500
m	.0368 lb./in.	.0368
Removable Blade Wt.	3.04 lb.	3.24
First Mass Moment	101.3 lb.-in.	107.5

The blade instrumentation consists of chordwise, flapwise and torsion strain gage bridges at 5 radial stations. The strain gages are located in depressions of the blade surface which are subsequently filled to preserve a smooth airfoil contour. Wiring is carried out through the fiberglass conduit and a slip ring.

4. MODEL ROTOR DYNAMICS

To achieve dynamic similarity of the model rotor, several design iterations had to be performed. As discussed in Section 3,

considerable effort was spent in reducing the weight of the rotor hub and the flapping hardware without compromising the loads criteria. Frequency placement was used to guide the design.

A comparison between the modal frequencies for the isolated model and full scale AAH rotor is given in Figure 5. These data assume all hub impedances to be infinite. Except for the torsion mode it can be seen that the model blade mode frequencies closely match those of the full scale blade. Note that the nondimensional flap bending frequencies of the model rotor are slightly lower than full scale values. This is a direct result of the heavier flapping hardware. Also, because of the increased inplane stiffness of the strap pack it is seen that the frequency of the first chord bending mode is slightly raised for the model rotor. However, these differences are minor, less than 0.1 rev., even for the high frequency elastic bending modes.

Without involving GRMS hardware, the only way to match torsional frequency was through changes in the model pitch link stiffness. Retaining the ideally scaled AAH pitch link stiffness would have resulted in a first torsion mode frequency at about 5.6/rev. The softest practical pitch link would have resulted in a torsional resonance at 5/rev. The full scale AAH has a first torsion mode frequency of about 4.7/rev. Because of this, it was decided to make the pitch link stiffness such that the torsional frequency was above, and well separated from, 5/rev. Since with this model blade torsional frequency both the model and full scale frequencies are separated from 5/rev., above and below respectively, it is not expected that the forced torsional responses will be signficantly different.

The model rotor is thus substantially dynamically similar to the full scale AH-64 main rotor. Studies of the model rotor dynamic and aeroelastic behavior could therefore be limited to a few basic cases. The dynamic Analysis Research Tool program (DART), a finite element program with special emphasis on rotor analysis, was used in these studies.

5. COUPLED MODEL ROTOR/GRMS VIBRATION AND LOADS

To permit analysis of the fully coupled rotor/GRMS system, certain dynamic properties of the GRMS had to be known. Since these data were not available, HHI defined the requirements and participated in a shake test of the GRMS at the NASA Langley V/STOL facility. Complete details of this test are contained in Reference 5.

Briefly, the data that are required for the analysis are the frequencies, generalized masses, generalized dampings, and modal

components of motion at the main rotor hub for all GRMS modes within a specified frequency range. The GRMS was tested with the fuselage and rotor removed, see Figure 6. A simulated hub weight was attached to the drive shaft. The structure was excited laterally and longitudinally at the hub using random forcing with a frequency range of 0 to 100 Hz. This range embraces the important rotor inplane cyclic modes and rotor 4/rev. Acceleration measurements at eighteen points on the GRMS structure were used to plot and identify the various GRMS modes. Linear and angular acceleration measurements at the hub were used to define the modal data needed for the analysis. These data showed that the hub impedance of the GRMS and the full-scale AH-64 are significantly different with respect to the ground resonance dynamics (modes below 1/rev.), the drive shaft bending dynamics, and the control system stiffness.

From the shake test data it is seen that the frequencies of the principal GRMS modes are separated from 1/rev. and 4/rev. within the normal operating rotor speed range. Similarly, the isolated blade frequency data provided in Section 4 show that the blade modal frequencies are separated from the rotor speed multiples. Coupling the model rotor to the GRMS can influence the blade and GRMS modes and thereby affect rotor loads and system vibration. An assessment of these effects was made by examining the modes for the fully coupled rotor/GRMS system.

Neglecting drive system torsional dynamics, the results of a fully coupled rotor/GRMS analysis showed that blade collective modes were unaffected and that the cyclic modes were only slightly influenced. Comparison with full scale AAH data showed that frequency matching is generally good except for the torsion mode, as noted in Section 4, and the chord bending mode. The reason for the lowered chord bending frequency is coupling with the high effective mass GRMS shaft bending modes. For this same reason the heavier than ideally scaled hub of the 27% scale model does not appreciably change frequency placement of the rotor modes. Because the coupling of the rotor to the GRMS has not substantially degraded the separation of the blade modal frequencies from the rotor harmonics, it can be concluded that the forced response characteristics of the blades will likewise be little affected.

Depending on their relative values, the weight and inertial properties of the rotating blades can influence the GRMS modes. High rotor to GRMS effective mass/inertia ratios generally lead to stronger coupling. This has implications for stability (in particular ground resonance discussed in Section 7) and forced response. Comparison of the uncoupled GRMS mode frequencies and those for the fully coupled rotor/GRMS system showed that the

fundamental GRMS modes are not appreciably changed through coupling with the rotor. Amplification of rotor loads is, therefore, expected to be minimal, resulting in low GRMS vibrations. Hub vibratory motions should likewise be low and have little influence on the blade response characteristics.

6. AEROELASTIC STABILITY AND LOADS

It was shown in Section 5 that coupling has little effect on the rotor and GRMS frequencies. This indicates that there is insignificant coupling between the rotor and the GRMS dynamics, apart from ground resonance. The addition of aerodynamic forces to the blades will not substantially alter this coupling, but they will influence the behavior of the blades themselves. Because the rotor to GRMS coupling is weak, the aeroelastic characteristics of the blades can be determined from isolated blade analyses.

Blade aeroelastic stability as a function of forward speed was studied at rotor speeds of 80%, 100% and 110% nominal. Forward speed was accounted for by applying aerodynamic forces corresponding to the 90-degree azimuth position. Results for the blade modal damping values showed that adequate stability margins are available. Studies of this type, with the rotor in an axial flow mode of operation, will generally identify inherent design flaws that would lead to aeroelastic instabilities in forward flight in the pitch-lag, pitch-flap, and flap-lag categories. It was apparent that the model rotor is not susceptible to any of these, which indicates a degree of aeroelastic similarity with the parent full-scale AAH rotor which has been demonstrated to be free from instability.

The chordwise relationship among the elastic axis, center of pressure, and center of gravity for the model blades is similar to that of the full scale blades. The model blade torsional frequency is only slightly higher than full scale. These facts permit the conclusion that the model rotor will be free from advancing blade flutter and static torsional divergence for flight conditions representative of the full-scale AAH main rotor.

Blade dynamic loads were studied next by comparing the radial distribution of half peak to peak loads for the model rotor with full-scale AH-64 loads from flight tests and analysis. Model blade moments were scaled up (by a factor of S^{-3}) in order to be directly comparable with full-scale results. Analytically obtained flapwise and chordwise bending moments in level flight were essentially the same for the full-scale and the model rotor. Torsion loads were approximately 20% higher for the model rotor.

This difference can be directly attributed to the higher control system and blade torsional stiffness of the model rotor. The comparison of model rotor and full-scale flight test bending moments for a 2.5g maneuver, Figure 7, shows excellent correlation. It is not anticipated that such a maneuver will be conducted in the wind tunnel; the data are provided only to give an indication of the capabilities of the AH-64 rotor and to show comparison with flight test data.

The blade load results presented here show that dynamic similarity has been achieved within the given constraints. Model blade bending loads can be directly scaled to full-scale values.

7. AEROMECHANICAL STABILITY

Possibly the most fundamental instability associated with rotorcraft is ground resonance, or, in more general terms, aeromechanical instability. This phenomena is, in fact, not a resonance but a true instability which can occur on the ground (even in vacuum) or when airborne. Mechanical stability of model rotors is of particular concern since it is not possible to 'fly out' of a problem as is generally the case with an actual rotorcraft. Ground resonance, as a mechanical instability in articulated rotor, is well understood. The classical works of Coleman and Feingold, and Deutsch identified the rotorcraft parameters and their relationships in defining this instability. In simple terms, mechanical instability can occur if: 1) The blade lag frequency is less than the rotor speed (soft inplane); 2) The lag frequency minus the rotor speed approaches, or coalesces with, the frequency of a fixed system mode and; 3) Certain relationships among the blade lag damping and airframe modal damping, and the effective rotor mass and airframe modal mass are satisfied.

For the scaled model AAH main rotor, the blade lag frequency is less than the rotor speed for operating rotor speeds above 40% nominal (40% N_R). Therefore, to integrate the rotor with the GRMS, mechanical stability must be considered. What follows describes the studies that were conducted to define and understand the stability characteristics. All results shown here were computed using the E-927 computer analysis[6].

Initial studies duplicated the classical model. That is, the blades were assumed free to only lag, the hub was assumed free to only translate laterally (roll direction) and longitudinally (pitch direction), and air density was zero (vacuum). Blade lag damping was 9% critical at 100% N_R. This is the value that is used for the full-scale AH-64 when all dampers are operative. It corresponds to a lead-lag amplitude of 5^o at the regressing lag

frequency. The GRMS modes that are important for mechanical stability are the gimbal pitch and motor roll modes because their frequencies and effective masses, see Table 5, are within the ranges of concern. The vertical and lateral sting bending mode frequencies are sufficiently low, and the effective masses sufficiently high to reduce the rotor to GRMS coupling to insignificant levels.

Table 5: GRMS Modal Properties

	Mass $lb\text{-}sec^2/in$	Frequency Hz	Damping % Critical	Hub Motion Linear	Hub Motion Angular
Gimbal Pitch	.402	12.0	13.7	1	.074
Motor Roll	.106	8.9	5.4	1	.063

Mechanical stability characteristics of this simplified system are shown in Figure 8. It can be seen that unstable coupling between the regressive lag mode and the GRMS motor roll mode is predicted to occur between 87% N_R and 104% N_R. It is also shown in this figure that the system can be stabilized by doubling the roll mode damping to 10.9%. Taken at face value, these results suggest that a further small increase in the roll mode damping would provide an adequate stability margin. It will be shown that this conclusion is erroneous and that more refined analysis is required to determine the stability characteristics of the coupled rotor/GRMS system.

The classical analysis described above addressed the purely mechanical instability known as ground resonance with a simplified model of the rotor and airframe (GRMS). Such simplified modeling has often proved to be adequate when applied to actual rotorcraft with articulated rotors, but there are circumstances under which this approach is quite inadequate. The model rotor/GRMS system is one such case.

For a typical rotorcraft, the ratio of the effective rotor mass to that of the airframe roll mode (which is generally of most concern) is normally less than 0.1. For the model rotor/GRMS motor roll mode this ratio is 0.3. Pitch or roll rotations of the hub that accompany hub translations in the important airframe modes of a typical rotorcraft are generally less than 0.02 radian/unit hub translation. For the GRMS, the roll and pitch rotations are respectively 0.063 and 0.074 radians/unit hub translation. A consequence of these rotations is that they cause blade flapping to participate much more in the model system than in typical rotorcraft. The primary influence of thrust on an

actual rotorcraft is to cause it to become partially, or wholly, airborne. Depending on the airframe modal properties, this can either degrade or improve stability. However, the effects are mainly due to changes in the dynamics of the airframe modes; thrust per se has only a minor influence. On the other hand, the model system cannot become airborne and thrust can have a significant influence on stability depending on the degree and phasing of flapping participation. Because of these considerations, it was decided that the analytical model of the rotor/GRMS system should include blade flapping as well as lagging, correct representation of the modal hub motions of the GRMS, rotor blade aerodynamic forces, and thrust effects. Rather than include all of these features simultaneously, a step-by-step approach was taken so that individual effects could be examined. Note that results in the following discussions were developed with 10.9% critical damping of the motor roll mode.

The influence of adding aerodynamics, thrust, and flapping motions to the baseline system is shown in Figure 9. When compared to Figure 8, these factors are seen to have little influence on stability. Introducing aerodynamics alone essentially has only the effect of adding profile drag to the blades. This will be small compared to the blade damping from the lag dampers. Therefore, the in vacuo and in air characteristics are similar. Increasing thrust adds induced drag which can be expected to augment lag damping and improve stability. Flapping is seen to have little influence on stability. In the absence of coning (zero thrust), the only forces that cause the blades to flap result from blade angle of attack changes due to blade lag and hub inplane velocities. These velocities are small compared to those from rotor speed. Consequently, flapping will be small. Therefore, the addition of the flapping degree of freedom has a negligible effect on stability. As the blades come under thrust, flapping caused by hub inplane accelerations will be induced by inertia forces on the coned blades. To illustrate the system behavior, the mode shape for the 1g thrust (1060 lbs.) configuration at the point of minimum stability is shown in Figure 10. This shows that the pattern of the blade lag motions is that classically associated with ground resonance. That is, the center of gravity of the rotor when viewed from above is moving in a retrograde sense in rotating axes -- opposite to the direction of rotor rotation. The instant in time shown is when the lateral (roll) flapping is maximum. Flapping causes the thrust vector to tilt through an angle equal to the flapping angle, thereby introducing a component acting in the plane of the hub. This component of thrust acts against the hub velocity, and provides a measure of positive damping. However, this is somewhat reduced by the Coriolis forces from blade flapping which provide negative damping. For the mode under consideration, all of these effects

are relatively small because the flapping participation is small (flapping is only about one-tenth of the lag amplitude), therefore the stability characteristics are similar to those for the system in Figure 8. The mode shape does, however, illustrate how factors other than those classically considered can enter into the picture.

The influence of adding a flapping degree of freedom and allowing the hub to pitch and roll while translating longitudinally and laterally, respectively, is shown in Figure 11 for a vacuum environment. Two effects are seen. First, the roll frequency increases with increasing rotor speed which causes coalescence with the regressive lag mode to occur at a higher rotor speed. Second, the system is destabilized. Part of the destabilizing influence can be traced to the fact that the blade lag damping constant is held constant with rotor speed. This means that the percent critical lag damping decreases with increased rotor speed. Also, damping required for stability increases as the coalescence rotor speed increases, largely due to the increased rotor energy available. It should be pointed out that the effect observed here is significant only because the GRMS has an unusually high rotor to roll mode effective mass ratio and unusually large hub rotations that accompany lateral motions of the hub in the roll mode. The flapping hinge offset is low, resulting in a nondimensional flap frequency of 1.02. These features of the model system make it more sensitive to the hub moments caused by blade flapping than would be the case for a typical rotorcraft with a similar low flap frequency.

The combined influence of aerodynamics, thrust, flapping degree of freedom, and hub pitch and roll is shown in Figure 12. Two effects are seen. First, increasing thrust increases the frequency separation between the roll and regressing lag mode at coalescence. This indicates a stronger coupling between these modes and, typically, a lesser degree of stability. Second, the system is destabilized in proportion to the amount of thrust developed by the rotor. For 9% critical lag damping and 1g thrust (1060 lbs.) the system is unstable for rotor speeds above $92\%N_R$.

The mode shape for this configuration at the point of minimum stability is shown in Figure 13. From this it is seen that the source of negative damping comes directly from thrust. Examining the phasing between flapping and rolling proves this point. The instant in time shown is when the lateral (roll) flapping is maximum. The thrust vector, being perpendicular to the tip path plane, thus tilts through an angle equal to and in phase with the flapping angle. The resulting thrust component in the plane of the hub acts in phase with the hub inplane velocity and thus provides a destabilizing force. The measure of negative

damping is directly proportional to the flapping amplitude and the amount of thrust. Comparing Figure 13 with 10 shows that the phasing between flapping and hub lateral motion is changed unfavorably when the hub rotational degrees of freedom are included. These studies are evidence that a simplified model does provide erroneous results in the situation at hand.

Another point to be made from Figure 12 is that a proper estimate of blade lead-lag damping is crucially important. For 20% critical blade lag damping the system is seen to be stable for 1g and slightly higher thrusts. The elastomeric damper properties are highly nonlinear functions of the lead-lag motion amplitude and its frequency content. Critical damping of 9% corresponds to 5^{o} lag amplitude at the regressing lag frequency. For 1^{o} lag amplitude at the regressing lag frequency critical blade lag damping would be 20%. Presence of lead-lag motions at other frequencies reduces blade damping in the ground resonance mode. Therefore, the blade lead-lag frequency response must be closely observed during testing to obtain a proper estimate of blade lag damping for the model rotor.

From Figure 12 it is evident that the 27% scale AH-64 rotor/GRMS system has considerably lower stability margins than the full-scale AH-64, which has been shown to be stable for reduced blade and fuselage damping values. Furthermore, there is considerable likelyhood that the model system will be unstable at operating RPM. A series of investigations was therefore performed to identify possible changes of the system parameters that would eliminate such an instability. Since it is desirable to maintain the model rotor properties as closely as possible to those of the full-scale rotor only GRMS changes were considered. By design, the GRMS roll and pitch springs and dampers can be varied. Consequently, the effect of these parameters was studied. The results can be summarized as follows. Changes to the GRMS pitch frequency and damping have little effect. This is not surprising, since it is the roll mode that couples with the regressing lag mode. Any increase in GRMS roll mode damping will be helpful, see Figure 14a. A considerable increase in roll frequency (above 1.5 * nominal) would be required to provide sufficient stability margins, see Figure 14b. A decrease in roll frequency would have been more effective. However, experience from the GRMS shake test showed that increasing the GRMS damping is accompanied by an increase in the corresponding frequency. A possible solution to the ground resonance instability would therefore consist of increasing the GRMS roll mode damping and frequency. It should be pointed out here that proper steps for a safe integration of the model rotor with the GRMS were taken by Langley personnel before wind tunnel testing commenced.

8. SUMMARY

A 27% Mach scaled model AH-64 rotor was developed at HHI for testing in the NASA Langley V/STOL tunnel with the GRMS test stand.

The design was guided by analysis to insure dynamic and aeroelastic similarity of the model with the full scale parent. The demanding requirements of Mach scaling dictated the use of advanced composite materials for the rotor blades.

A ground resonance instability at operating RPM is predicted. This instability is due to the combined effects of thrust and lack of "fly-away" capability. This adverse effect is amplified by the high ratio of effective rotor mass to that of the GRMS roll mode and the large GRMS roll rotation per unit hub lateral translation. Close attention must be paid to these factors when integrating any model rotor with a test stand.

A solution to the ground resonance problem is projected using the unique GRMS features to change the fixed system properties.

The AH-64 model rotor has been tested safely and successfully in the V/STOL tunnel to obtain performance and blade loads data. It will be a useful tool for future research.

REFERENCES

1. Wilson, J.C., "A General Rotor Model System for Wind-Tunnel Investigations", J. Aircraft, Vol. 14, No. 7, July 1977, pp. 639-643.

2. Amer, K.B. and R.W. Prouty, "Technology Advances in the AH-64 Apache Advanced Attack Helicopter", Proc. of the 39th Annual AHS Forum, May 1983, pp. 550-567.

3. Bingham, G., "The Aerodynamic Influence of Rotor Blade Airfoils, Twist, Taper, and Solidity on Hover and Forward Flight Performance", Preprint No. 81-4, Proc. of the 37th Annual AHS Forum, May 1981.

4. Keys, C.N., et al., "Considerations in the Estimation of Full-Scale Rotor Performance from Model Rotor Test Data", Proc. of the 39th Annual AHS Forum, May 1983, pp. 34-43.

5. Straub, F.K., "NASA Langley Research Center General Rotor Model System Shake Test Report", Hughes Helicopters Report No. 150-V-1002, November 1981.

6. Johnston, R.A., "Rotor Stability Prediction Correlation with Model and Full-Scale Tests", Preprint No. 931, Proc. of the 31st Annual AHS Forum, May 1975.

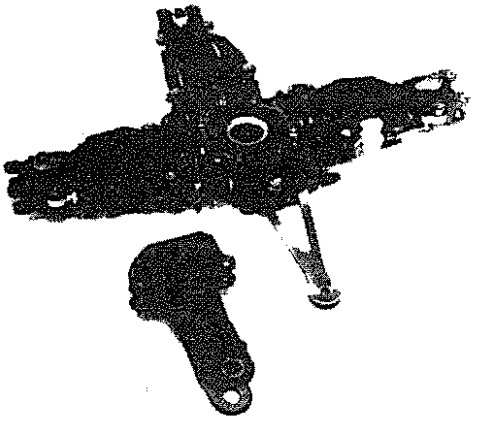

Fig. 1: 27% Scale Model AH-64 Main Rotor Hub.

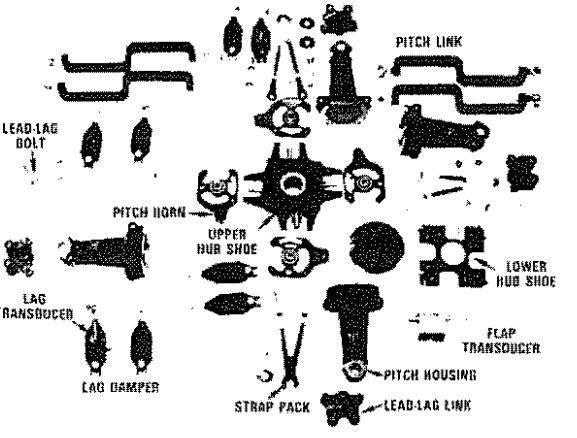

Fig. 3: Model Hub Components.

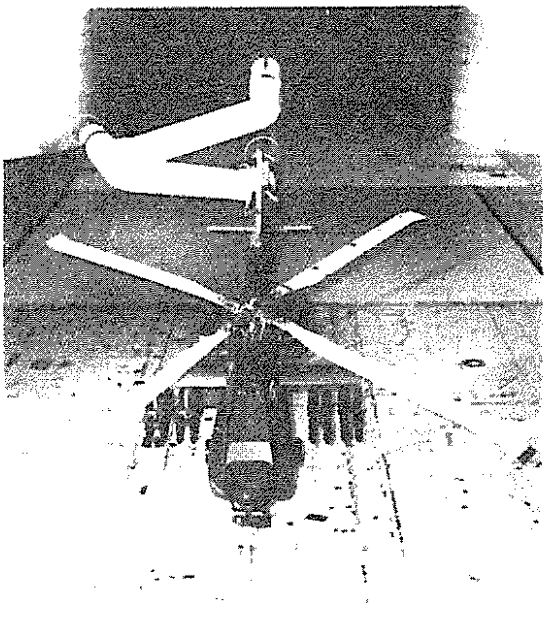

Fig. 2: 27% Scale Model AH-64 in NASA Langley V/STOL Wind Tunnel.

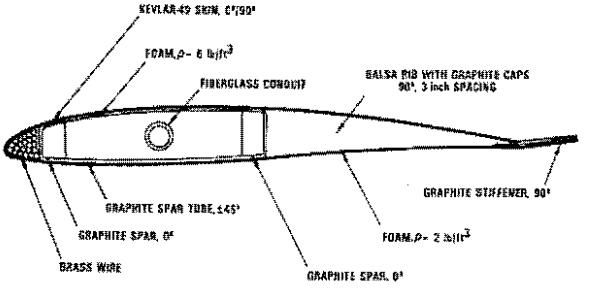

Fig. 4: Model Blade Cross-Section.

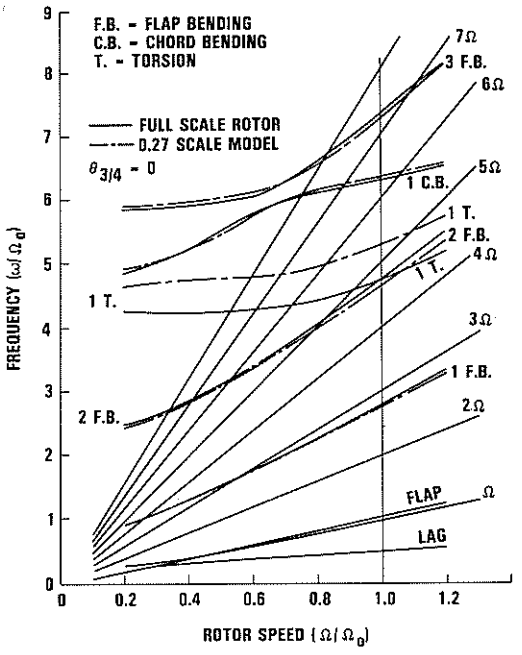

Fig. 5:

Isolated Blade Resonance Diagram, Model Rotor Versus Full-Scale.

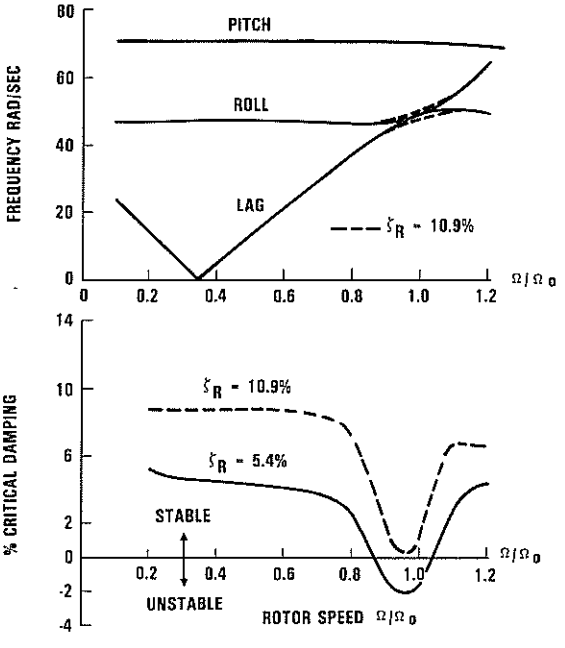

Fig. 8: 27% Scale Rotor/GRMS Ground Resonance, Classical Model (in Vacuum, Lag and Hub Translation Degrees of Freedom).

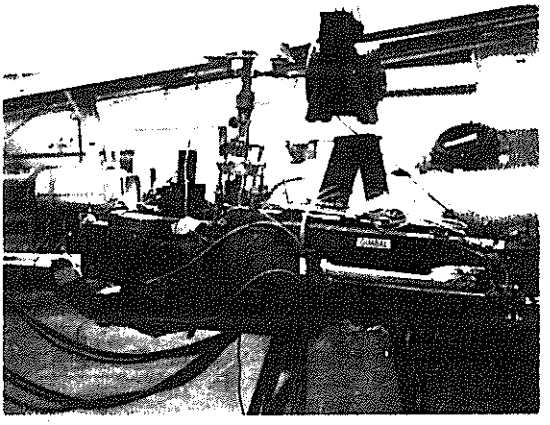

Fig. 6: General Rotor Model System During Shake Test.

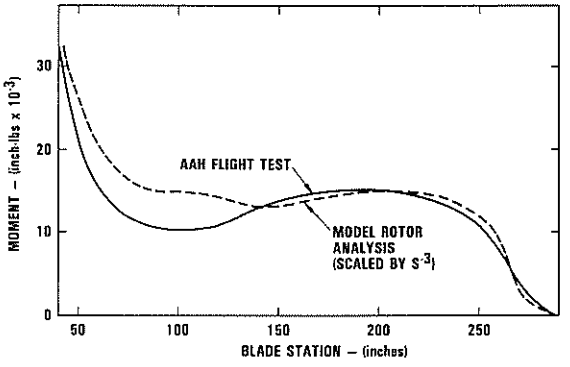

Fig. 7a: Flapwise Blade Bending Moment Versus Radius (½PP, 164 knots, 2.5g Maneuver).

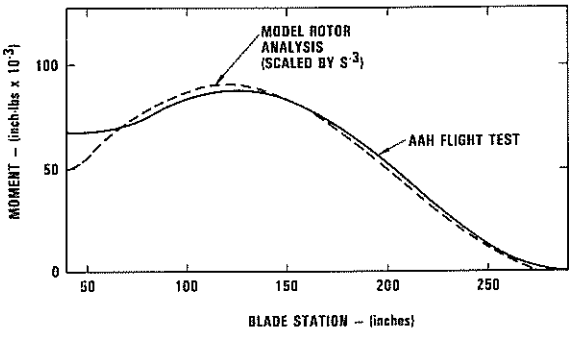

Fig. 7b: Chordwise Blade Bending Moment Versus Radius (½PP, 164 knots, 2.5g Manuever).

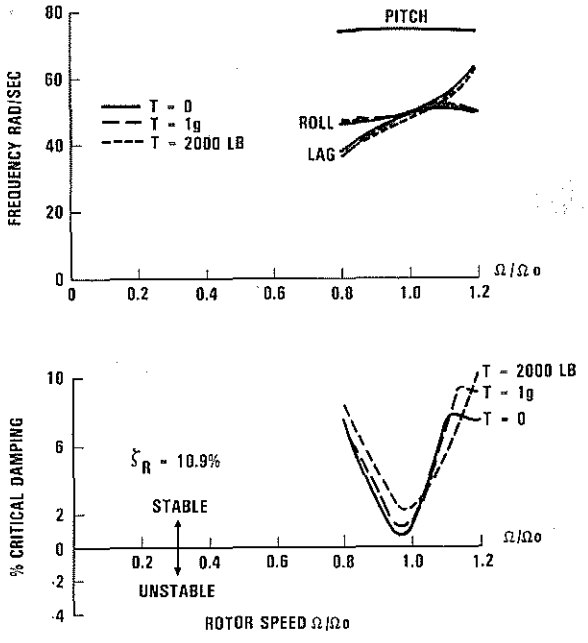

Fig. 9: Effect of Rotor Thrust and Flapping on Ground Resonance Stability (Lag, Flap, Hub Translations).

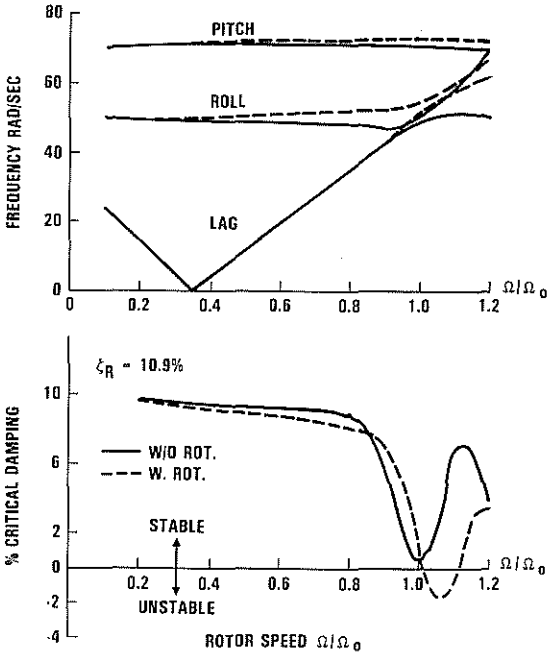

Fig. 11: Effect of Hub Rotations on Ground Resonance Stability (in Vacuum, Lag, Flap, Hub Translations).

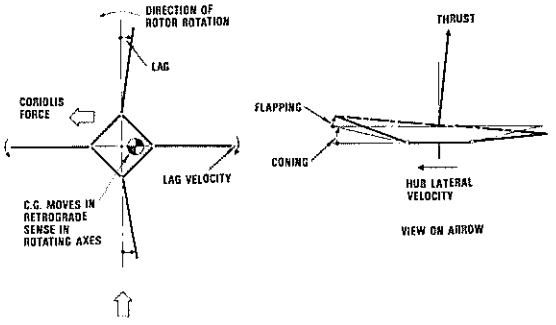

Fig. 10: Ground Resonance Mode Shape Without Hub Rotations (1g Thrust).

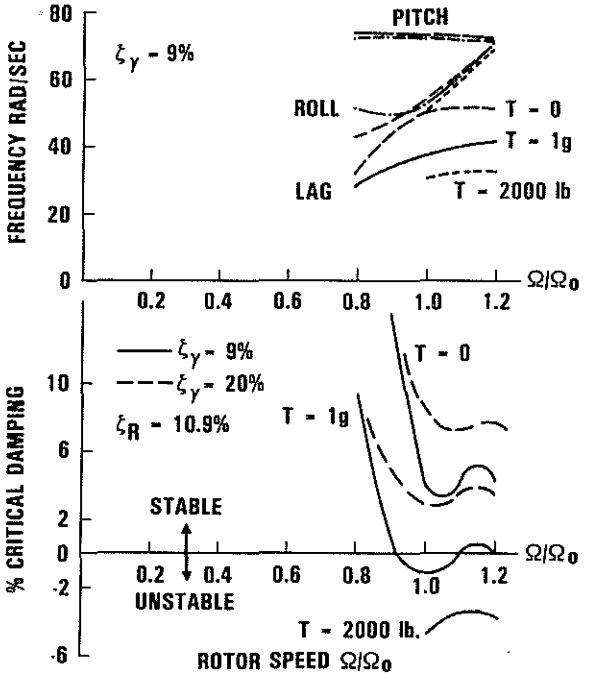

Fig. 12: Effect of Hub Rotations and Thrust on Ground Resonance Stability. (Lag, Flap, Hub Translations and Rotations).

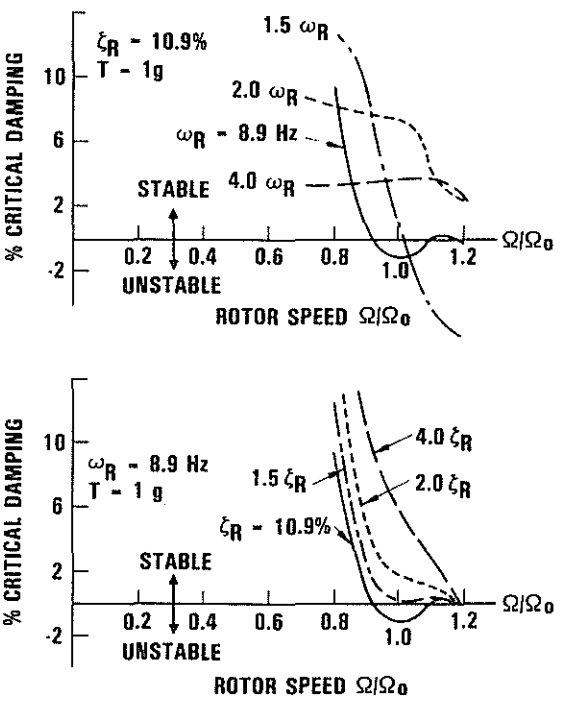

Fig. 14: Projected Solution of Ground Resonance Instability Through Increased Roll Damping and Frequency. (Lag, Flap, Hub Translations and Rotations).

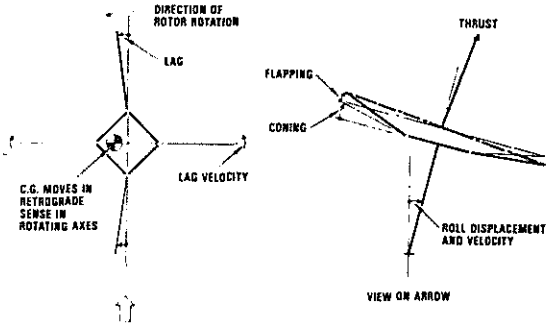

Fig. 13: Ground Resonance Mode Shape With Hub Rotations Included (1g Thrust).